Journal of Physics:
Conference Series

PAPER • **OPEN ACCESS**

Enhancing Earth-Mars Transfer Trajectories: A Conic Patch Method Using Evolutionary Algorithms

To cite this article: A.M. Abdelaziz and S.K. Tealib 2025 *J. Phys.: Conf. Ser.* **3070** 012019

Journal of Physics: Conference Series **3070** (2025) 012019 doi:10.1088/1742-6596/3070/1/012019

Enhancing Earth-Mars Transfer Trajectories: A Conic Patch Method Using Evolutionary Algorithms

A.M. Abdelaziz [1*], S.K. Tealib [1]

[1] National Research Institute of Astronomy and Geophysics (NRIAG), Helwan, Egypt.

[*]E-mail: ahmed_astro84@nriag.sci.eg

Abstract. Given the importance of interplanetary transfers in celestial mechanics, this paper introduces a novel patched-conic method for designing interplanetary orbits, providing an optimized framework for mission planning. The transfer problem is formulated by identifying key parameters such as launch windows, transfer angles, and delta-v requirements, which are optimized using an evolutionary algorithm to minimize fuel consumption and flight duration. The study employs consecutive solutions to Lambert's problem, focusing on the intersection points of conic sections to calculate the total transfer cost. The proposed method demonstrates rapid convergence, making it highly suitable for computational implementation and practical mission planning. This study presented an optimized interplanetary trajectory for a spacecraft traveling from Earth to Mars using the Particle Swarm Optimization (PSO) algorithm. The results successfully demonstrate the capability of PSO to minimize the total Δv required for the mission while ensuring adherence to mission constraints and achieving efficient flight times.

1. Introduction

Interplanetary trajectory design is a cornerstone of space exploration, requiring precise modeling and optimization of spacecraft paths. The patched-conic method has emerged as a foundational approach in this domain, offering a practical and computationally efficient approximation of precise orbits. As highlighted by [1], this method divides a spacecraft's trajectory into a sequence of two-body problems, simplifying the complexities inherent in multi-body dynamics while maintaining the accuracy required for mission planning and trajectory optimization.

Traditional transfer techniques, such as Hohmann transfers [2] and bi-elliptic transfers [3], prove effective in specific scenarios but often face limitations in efficiency and flexibility, particularly in complex mission architectures [4]. These methods are less adaptable to multi-target or long-duration missions, where a higher degree of versatility is essential to meet diverse objectives and constraints [5]. The patched-conic method addresses these challenges by segmenting the spacecraft's path into interconnected conic sections—each governed by two-body dynamics—providing a versatile framework for designing and optimizing interplanetary trajectories [6]. Planning an interplanetary mission using the patched-conics method simplifies the complex task of spacecraft trajectory planning by dividing it into manageable, interconnected segments [7]. The first stage is Interplanetary Exit: The spacecraft begins in a stationary orbit around its originating planet (e.g., Earth). A speed increase, typically achieved through a rocket

burn, transitions the spacecraft from this stationary orbit into a hyperbolic escape trajectory, allowing it to exit the planet's gravitational influence and enter an interplanetary transfer orbit. The second stage is Interplanetary Entry: As the spacecraft approaches its destination planet, it reduces its speed, again typically through a burn, to transition from a hyperbolic approach trajectory into an orbit around the target planet. This process requires the spacecraft to adjust its speed appropriately to ensure successful capture into orbit.

A critical element in trajectory design is solving Lambert's problem, a classical two-point boundary value problem (TPBVP) introduced by Johann Heinrich Lambert in the 18th century [8]. Lambert's problem focuses on linking two specified positions in space over a given time of flight using ballistic, conic arcs. It is crucial for determining the time required for a spacecraft to travel between two points along a defined trajectory. Lambert's theorem states that the transfer time depends solely on the sum of the position vectors, the distance between the points, and the semi-major axis of the trajectory. This provides a foundation for calculating the necessary velocity changes (delta-v) for transfers, making it a cornerstone of orbital maneuver optimization [9]. Building on these principles, the patched-conic method simplifies interplanetary trajectory design by approximating a spacecraft's path as a sequence of conic sections connected at transition points: First Conic: Represents the spacecraft's initial stationary orbit around the originating planet. Second Conic: Models the hyperbolic escape trajectory as the spacecraft departs the sphere of influence of the originating planet. Third Conic: Describes the heliocentric transfer orbit directing the spacecraft toward the target planet. Fourth Conic: Represents the approach trajectory as the spacecraft nears the target planet and transitions into its sphere of influence. Fifth Conic: Defines the final orbit the spacecraft assumes around the target planet upon gravitational capture. This structured segmentation offers a clear and manageable way to model spacecraft trajectories, enabling accurate and efficient mission planning. It bridges the gap between simplistic two-body problems and the complexities of multi-body dynamics while allowing the integration of advanced optimization techniques, such as evolutionary algorithms, to minimize fuel consumption, delta-v requirements, and travel time.

This study proposes an enhanced patched-conic method for interplanetary trajectory design, integrating Lambert's problem into the framework to optimize trajectory parameters further. By addressing the challenges of modern space exploration, the proposed method advances adaptability, improves computational efficiency, and enhances mission success.

2. Lambert algorithm for transit orbit

In interplanetary trajectory design, the transfer orbit typically constitutes the majority of the mission duration. To determine this critical segment of the trajectory, the Lambert algorithm is employed. This algorithm calculates the transfer orbit using two specified position vectors (the departure and arrival positions) and the transfer time between them. The departure position is defined at the boundary of the sphere of influence of the originating planet, while the arrival position is located at the boundary of the sphere of influence of the target planet. As an initial approximation, the total mission time estimates the transfer time. However, the precise determination of these parameters departure and arrival positions, transfer time, and associated orbital characteristics forms the core of the proposed method [1].

The ability to accurately refine these coefficients ensures optimal trajectory design, minimizing fuel consumption and mission duration while maintaining robust adaptability to diverse mission requirements. This proposed approach integrates advanced computational techniques with the Lambert algorithm to achieve high-precision solutions for interplanetary

transfers. Lambert's theorem is a fundamental principle in astrodynamics, used to determine the transfer time between two points, $\boldsymbol{P_1}$ and $\boldsymbol{P_2}$, along an orbital path. This is a critical aspect of spacecraft mission planning, particularly when transferring from one orbit to another [9]. The Lambert problem involves calculating a trajectory that connects two specified position vectors, $\boldsymbol{r}_E$ and $\boldsymbol{r}_O$, in a given time of flight Δt, assuming Keplerian motion. As illustrated in Figure 1 the primary body, F, acts as the gravitational center and origin of the reference frame. For interplanetary transfers, F typically represents the Sun, while for geocentric motion, it represents the Earth. At times t_1 and t_2 (where $t_2 > t_1$), the spacecraft occupies positions r_E and r_O, respectively. The transfer time $\Delta t = t_2 - t_1$ represents the duration of the motion between these two points. Additionally, the angle θ between r_E and r_O defines the trajectory's direction of motion [10]. Kepler's equation describes the relationship between an object's position along its orbit and the passage of time. Specifically, it helps to determine the difference in eccentric anomalies $(E_2 - E_1)$ over time between two points on an orbit. The equation incorporates the orbit's eccentricity e, a factor that characterizes how elliptical the orbit is, and the time difference $(t_2 - t_1)$ which can be expressed as [11]:

$$E_2 - E_1 - e(\sin E_2 - \sin E_1) = \sqrt{\frac{\mu}{a^3}}(t_2 - t_1) \tag{1}$$

We can express the equation in different forms:

$$\frac{a^3}{2}[\alpha - \sin\alpha - (\beta - \sin\beta)] = \sqrt{\mu}(t_2 - t_1) \tag{2}$$

where α and β are angles described by.

$$\alpha = 2\sin^{-1}\left(\sqrt{\frac{s}{2a}}\right), \beta = 2\sin^{-1}\left(\sqrt{\frac{s-c}{2a}}\right) \tag{3}$$

Equations (3) define the angles α and β in terms of the semi-major axis (a) and two additional parameters. One of these parameters, s is defined as half the sum of the distances between Earth and another object.

$$s = 0.5(r_E - r_O + c) \tag{4}$$

The parameter c represents the distance between two points based on their respective distances from a central body (such as Earth and an object) and the angle θ between them. This distance is typically calculated using the law of cosines, where θ is the angle formed between the

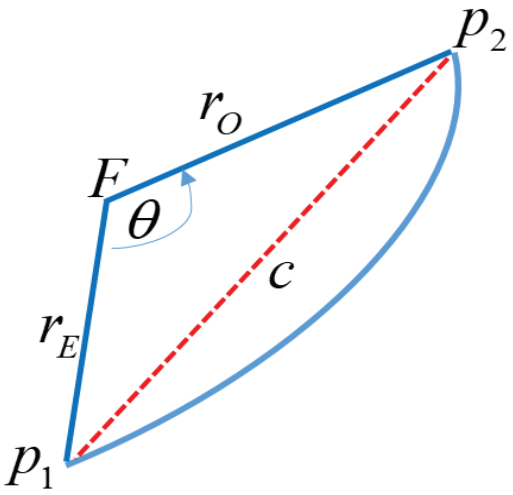

Figure 1. Definition of Lambert's Problem.

two positions vectors of the points relative to the central body. The relationship can be expressed as:

$$c = \sqrt{r_E^2 + r_O^2 + 2r_E r_O \cos\theta} \tag{5}$$

The fundamental equation relates the transfer time (Δt\Delta tΔt) to the geometry of the orbit

$$\Delta t = \frac{\sqrt{a^3}}{\mu}\left[2\,arcsin\sqrt{\frac{s-c}{2a}} - sin\,2\,arcsin\sqrt{\frac{s-c}{2a}}\right] \tag{6}$$

Using Lambert's equation, one can solve for the transfer times between orbits, which is crucial for planning spacecraft trajectories. The solutions can handle different types of orbits, such as elliptical or hyperbolic, depending on the energy involved. To solve Lambert's problem, initial conditions must be established by specifying the starting and ending points of the transfer. From there, the velocities at these points can be determined, allowing the calculation of the energy needed for the spacecraft to follow the planned trajectory [12].

enabling versatile applications from debris monitoring to collision risk mitigation in support of Space Situational Awareness (SSA) objectives [9]

3. Radius of the Sphere of Influence

In celestial mechanics, especially in problems involving close encounters, it is crucial to identify regions where one celestial body's gravitational influence dominates over others. This is achieved through the concept of the Sphere of Influence (SOI), which delineates the region around a celestial body, such as a planet, where its gravitational pull is more significant than external forces, like the Sun's gravity [13].

The SOI plays a pivotal role in spacecraft mission planning, serving as a reference for key trajectory transitions. For instance: Departure Phase: When leaving the initial planet, a spacecraft must increase its velocity to escape the planet's SOI. Exceeding the escape velocity allows the spacecraft to transition from the planet's gravitational influence into a heliocentric transfer trajectory. Gravity-Assist Maneuvers: During a planetary flyby for gravity assist, the SOI marks the region where the approaching planet's gravity becomes dominant. Within this zone, the spacecraft can exploit the planet's gravitational field to alter its velocity and trajectory efficiently. Arrival Phase: As the spacecraft approaches its destination planet, the SOI defines the transition from the Sun's gravitational dominance to that of the planet. This enables the spacecraft to be captured into orbit around the destination planet or to execute a controlled landing.

Understanding and accurately defining the SOI are essential for calculating critical mission parameters such as delta-v requirements, transfer trajectories, and orbital insertion strategies. This concept ensures precise navigation and enhances mission efficiency by leveraging gravitational interactions.

The radius of the Sphere of Influence (SOI) is a key parameter in celestial mechanics, defining the boundary at which a planet's gravitational pull becomes more significant than the Sun's gravitational influence. This parameter is crucial for planning spacecraft maneuvers, including entry into and exit from a planet's gravitational domain [14].

The SOI radius,r_{SOI}, can be calculated using the following equation:

$$r_{SOI} = r_p\left(\frac{m_p}{M_s}\right)^{\frac{2}{5}} \tag{7}$$

where r_p is the distance between the planet and the Sun (or the central body around which the planet orbits), m_p is the mass of the planet, and M_s is the mass of the Sun (or the central body).

The equation used to calculate the Sphere of Influence (SOI) determines the distance from a planet within which its gravitational pull surpasses that of the Sun. Within this radius, a spacecraft will primarily experience the planet's gravity, making it critical for planning interplanetary missions. This calculation helps define the region where the planet's gravitational influence is dominant, facilitating spacecraft trajectory planning, including escape maneuvers, gravity assists, and orbital captures. The SOI equation is essential for guiding spacecraft navigation and ensuring precise mission execution in the complex gravitational environment of the solar system.

$$r_{SOI} = 0.9431a\left(\frac{m_p}{M_s}\right)^{\frac{2}{5}} \tag{8}$$

where a: semi-major axis of the planet's orbit around the Sun (or the central body), and the constant 0.9431 is a coefficient that adjusts the formula for the specific context being considered.

4. Patched Conics Trajectory Overview

The angular representation in the patched-conics method plays a vital role in optimizing spacecraft trajectories. It enables mission planners to focus on the spacecraft's orientation and positioning at critical points in its journey, ensuring seamless transitions between different conic sections, such as Earth orbit, heliocentric transfer, and Mars orbit. The angular coordinates (θ_A, θ_B, θ_C, θ_D) denote the spacecraft's positions at key points in the trajectory relative to a chosen reference direction. These angles are measured counterclockwise from the reference direction as positive values and clockwise as negative values. The trajectory involves three key maneuvers, facilitating transitions between the spheres of influence (SOI) of Earth, the Sun, and Mars. As illustrated in Figure 2 the spacecraft starts from Earth's SOI at point A, transitions to a heliocentric orbit, and eventually enters Mars' SOI at point C. The angular positions at these points are critical for defining and optimizing the interplanetary transfer. These coordinates provide essential parameters for calculating transfer time, fuel efficiency, and precise orbital maneuvers. In the first maneuver, the spacecraft departs from a waiting orbit around Earth and reaches the boundary of Earth's Sphere of Influence (SOI). Point A represents the spacecraft's initial position within Earth's SOI, located at an altitude of 0.1 time Earth's radius and at a specific angle $\theta_A = \frac{\pi}{2}$.

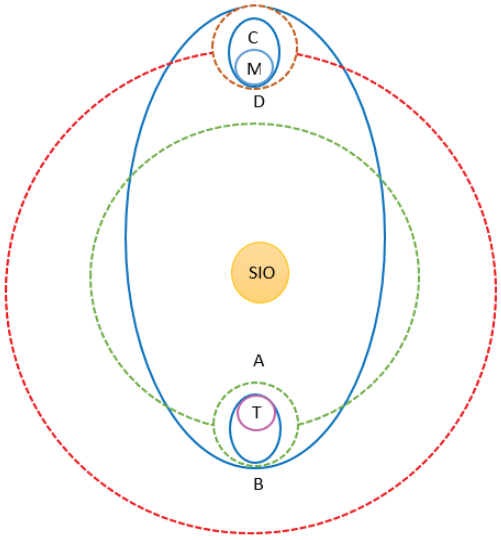

Figure 2. Simplified Representation of Free Parameters in Patched Conics Trajectory Analysis.

At this position, the spacecraft moves tangentially to Earth's orbit around the Sun, with the angle measured from a reference direction aligned with Earth's velocity vector in its heliocentric orbit. After completing this initial maneuver, the spacecraft exits Earth's gravitational influence and begins its interplanetary transfer towards Mars at a designated angle of $\theta_B = -\frac{\pi}{2}$. In the second maneuver, the spacecraft transitions from the edge of Earth's SOI to the boundary of Mars's SOI. Point B marks this transition, where the spacecraft leaves Earth's influence and follows an interplanetary transfer orbit. As the spacecraft approaches Mars, it begins to enter Mars's gravitational influence. In the third maneuver, the spacecraft moves from the edge of Mars's SOI to a waiting orbit around Mars. Point C indicates the spacecraft's entry into Mars's SOI at a specified angle of $\theta_c = \frac{\pi}{2}$. At this stage, an additional maneuver is required to transition into a stable Mars-centric orbit. Finally, Point D represents the spacecraft's position within Mars's SOI at an altitude of 0.3 Mars's radius and at a defined angle $\theta_c = \frac{-\pi}{2}$, signifying the successful completion of the interplanetary mission.

To accurately account for velocity differences at various stages of the mission, it is essential to recognize the shifting reference frames throughout the journey: the velocity at Point A is measured relative to Earth, at Point B relative to the Sun, and at Point C relative to Mars. Seven critical parameters are considered in this mission: four angular positions (A, B, C, D) and three time durations. First time duration: This represents the number of days required for the spacecraft to complete the initial maneuver, leaving Earth's gravitational influence and entering its interplanetary trajectory. Second time duration: This is the time required for the spacecraft's journey through interplanetary space, transitioning from Earth's SOI to Mars's SOI. Third time duration: This represents the time needed to execute the final maneuver, allowing the spacecraft to achieve a stable orbit around Mars upon entering its SOI. By carefully tuning these parameters, mission planners optimize the mission's overall cost, primarily measured by the total Δv, which directly correlates with fuel consumption. The angular positions determine the spacecraft's trajectory through space, while the time durations control the timing and speed of the journey. By optimizing these variables, mission planners ensure efficient fuel utilization, precise trajectory execution, and the successful transfer of the spacecraft from Earth to Mars.

5. Optimizing Orbital Transfers

In space dynamics, Particle Swarm Optimization (PSO) proves particularly effective for solving orbital transfer problems with high numerical precision [15]. Within this context, the Sphere of Influence is critical. The SOI defines the region around a celestial body, such as a planet, where its gravitational influence outweighs other forces, such as the Sun's gravity. The concept of is integral to several key mission phases:

- Spacecraft Departure: The spacecraft must accelerate to escape the planet's SOI and enter an interplanetary transfer trajectory.

- Planetary Approach for Gravity Assist: The spacecraft utilizes the SOI to exploit the planet's gravitational field, modifying its trajectory to achieve the desired course.

- Orbital Capture at the Destination: The SOI signifies the transition from a heliocentric orbit to the planet's gravitational domain, enabling the spacecraft to enter and stabilize in orbit around the target planet.

By incorporating PSO, mission planners can optimize critical parameters, such as Δv transfer times, and trajectory angles, while ensuring the spacecraft transitions smoothly through different spheres of influence [16]. This capability makes PSO a powerful tool in modern astrodynamics. The PSO algorithm operates with a user-defined number of particles, denoted by "n" Each particle represents a unique state among the possible program inputs, corresponding to a vector of seven unknown parameters. These parameters are constrained within user-specified upper bound (UB) and lower bound (LB) values. The seven unknowns are the parameters described in the previous section. Once the values for n, UB, and LB are set, the PSO algorithm randomly generates n particles, each represented as a vector of seven unknowns, with values randomly selected within the defined bounds. The algorithm begins by applying a cost function to each particle, calculating a corresponding cost value. Then, the iterative process begins, with the user specifying the number of iterations i. During this phase, the algorithm directs the particles toward the local minimum while maintaining diversity, allowing each particle to explore new regions and potentially discover a minimum close to the global minimum of the cost function. This is achieved through a velocity function, which assigns movement values to each particle, determining the distance a particle moves from its previous position based on its proximity to potential minima. In the first iteration, the velocity function is initialized with a random value, as outlined in Equation 9 [17].

$$v_{i+1} = \omega\, v_i + \phi_p r_p(\mathrm{b}_i - \mathrm{x}_\mathrm{i}) + \phi_g r_g(b_g - x_i) \tag{9}$$

where x_i is the particle's current state, a vector with seven elements), v_i is the velocity vector, while b_i is the best state that particular particle has found so far, and b_g is the best state discovered among all particles. The term $\boldsymbol{\omega}$ refers to the inertia weight, which prevents drastic changes in velocity from one iteration to the next. The cognitive Parameter $\boldsymbol{\phi_p}$ is a user-defined value between 0 and 1 that influences the particle's velocity based on how close it is to its personal best position. Similarly, the social parameter also a user-defined value between 0 and 1, determines the velocity's dependence on the particle's proximity to the global best position.$r_{p,}$ and r_g are random values between 0 and 1 associated with the cognitive and social parameters, respectively, introducing variability in how the particle responds to local and global solutions during each iteration.

Equation 9 can be analyzed by breaking it into three terms. The first term,ωv_i represents the inertia of the velocity, helping to prevent drastic changes in velocity from one iteration to the next, thereby maintaining stability. The second term, $\phi_p r_p(\mathrm{b}_i - \mathrm{x}_\mathrm{i})$, reflects the particle's tendency to

move toward its personal best position; as the particle gets closer to its historical minimum, its velocity decreases, making it more likely to remain near that local minimum. The third term, $\phi_g r_g(b_g - x_i)$ represents the particle's attraction to the global best position, with the velocity decreasing as the particle approaches the global minimum, encouraging convergence toward the best solution found by all particles.

The particle is updated (iterated) according to Equation 9. This process is repeated *i* times, as specified by the user [18].

$$x_{i+1} = x_i + v_i \tag{10}$$

In this equation, x_{i+1}represents the updated position of the particle. This update process is repeated for iii iterations, as specified by the user. With each iteration, the particle moves to a new position based on its velocity, allowing it to explore the solution space in search of an optimal solution.

6. **Numerical simulation**

The Particle Swarm Optimization (PSO) algorithm was employed to assess the costs associated with implementing a transfer trajectory via the patched conics method, integrating Lambert's function for trajectory calculations. The process began with defining the upper bounds (UBs) and lower bounds (LBs) for each of the mission's variables. For this analysis, an Earth-to-Mars interplanetary mission was modeled, leveraging the patched conics technique with simplifications. The mission adopted Hohmann transfers for all three critical maneuvers previously described. The estimated flight times for the maneuvers were determined to be approximately 0.49 months for maneuver 1, 8.24 months for maneuver 2, and 0.87 months for maneuver 3.

The corresponding upper and lower bounds for the variables are summarized in Table 1 This setup provides the foundation for the PSO algorithm to optimize the trajectory while minimizing the associated costs. Table 1 shows the key parameters for the spacecraft's mission, including the four angles (A, B, C, and D) corresponding to critical points along the spacecraft's trajectory. Angle A represents where the spacecraft starts its escape maneuver in Earth's waiting orbit. Angle B marks the edge of Earth's Sphere of Influence, where the spacecraft transitions to an interplanetary trajectory. Angle C is at the edge of Mars' Sphere of Influence, just before the spacecraft enters Mars' gravitational field. Finally, Angle D represents the spacecraft's position in Mars' waiting orbit, marking the completion of its journey. The table includes the "Number of Days" for each phase of the mission: Number of Days 1 is the time it takes to travel from Earth's waiting orbit to the edge of the SOI, Number of Days 2 covers the interplanetary journey from Earth's SOI to Mars' SOI, and Number of Days 3 is the time it takes to move from SOI to Mars' waiting orbit. For the lower bounds, all angles (A, B, C, D) are 0 radians, meaning the spacecraft's position starts at a defined reference point. The lower bounds for the number of days are 0. For the upper bounds, the values of all angles are 2π radians (360 degrees), which represent a

Table 1. Upper and Lower Bounds for PSO Parameters.

	Angles A (rad)	Angles B (rad)	Angles C (rad)	Angles D (rad)	No. Days (1)	No. Days (2)	No. Days (3)
Lower Bound	0	0	0	0	0	0	0
Upper Bound	2π	2π	2π	2π	30	360	30

complete orbit, allowing flexibility in positioning. The upper limit for the number of days for Maneuvers 1 and 3 is 30 days

7. Results and discussion

This section presents pivotal data for analyzing and validating the optimized interplanetary trajectory. Table 2 shows the results obtained from various attempts to minimize the total cost involved in the trajectory studied through the optimization algorithm used. Here, we see different values for the total cost, which vary even for the same number of iterations. This is because there are minima, and the algorithm identifies a local one based on the available time (number of iterations) to evaluate the sample space. The table presents the positioning characteristics of each of the four points, generally representing one of the algorithm's executions, along with the flight time for each arc of the connected conic sections. The sum of these times gives the total flight time. Based on the results presented, the most optimized trajectory was found with a cost of Δv = 5.5037 km/s. This trajectory is characterized by points A, B, C, and D. The angular coordinates of these points are provided, representing the direction of Earth's trajectory relative to the Sun, within the orbital plane. The position vectors for these points, relative to the respective planets, are given in kilometers and describe their precise locations within the trajectory.

$$\vec{r}_{A,Eart\square} = (-7.04,3.76,0), \quad \vec{r}_{B,Eart\square} = (865.74,13.63,0),$$
$$\vec{r}_{C,Mars} = (-497.34,73.76,0), \quad \vec{r}_{D,Mars} = (2.54,-3.78,0)$$

Table 3 breaks down the orbital characteristics of each segment of the optimal trajectory. For each segment (AB, BC, CD), the orbital energy, angular momentum, semi-major axis, eccentricity, and rotation angle (φ) are provided. These metrics describe the spacecraft's motion within the connected conic sections of the trajectory. Table 4 provides critical details on the velocities at each trajectory point (A, B, C, D), including the arrival velocity (Varr), departure velocity (V^{dep}), and the required Δv for orbital impulses. These values indicate the spacecraft's dynamics and propulsion needs, offering a detailed picture of the mission's velocity budget.

Table 2. Optimized Trajectory Results from Iterative PSO Calculations.

Total Cost (km/s)	Angle A (rad)	Angle B (rad)	Angle C (rad)	Angle D (rad)	Days 1	Days 2	Days 3	Particles	Iterations
7.1000	2.5000	0.9000	4.5000	1.5000	25.0	260.0	22.0	500	200
6.9500	2.4500	1.0000	4.4000	1.6000	28.0	255.0	23.0	500	200
6.7000	2.5500	3.0000	6.0000	3.0000	27.0	260.0	22.0	500	200
6.6000	2.6000	2.9000	5.9000	2.9000	30.0	258.0	24.0	500	200
6.3000	2.5500	3.1000	5.8000	3.0000	29.0	260.0	23.0	500	200
6.1000	2.5000	3.0000	5.7000	2.8000	28.0	259.0	22.0	500	200
5.9000	2.4500	6.0000	5.8000	3.2000	29.0	260.0	22.0	500	200
5.7000	2.4000	6.1000	5.9000	3.1000	30.0	259.0	23.0	500	200
5.6000	2.4500	6.2000	6.2000	3.1000	28.0	260.0	24.0	5000	2000
5.5037	**2.4000**	**6.1000**	**6.0000**	**3.0000**	**27.0**	**258.0**	**23.0**	**5000**	**2000**

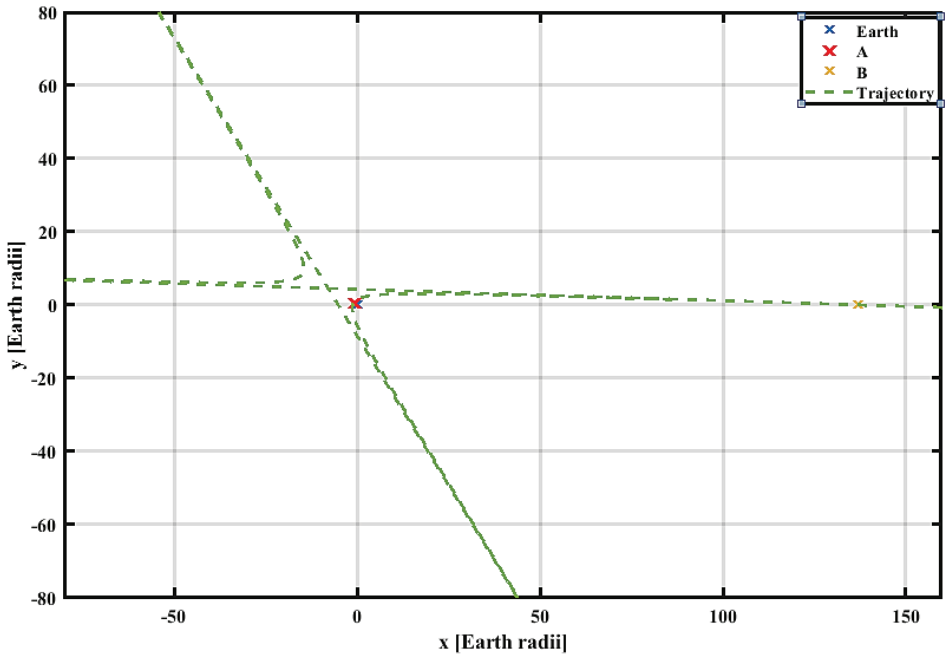

Figure 3. Trajectory in Earth's Reference Frame

Table 3. Characterization of the Connected Conic Sections for the Refined Trajectory.

Orbit	Energy [km^2/s^2]	Angular Momentum (h) [km^2/s]	Semi-major axis (a) [km]	Eccentricity (e)	Orbit Rotation(φ) [rad]
AB	3.7852	(0, 0, 7.6254e04)	-5.2284e04	1.1266	5.8569
BC	-351.5653	(0, 0, 4.7969e09)	1.9780e08	0.2068	1.7263
CD	3.4949	(0, 0, -2.2717e04)	-6.889e03	1.625	2.0326

Figures 3, 4, and 5 illustrate the optimized trajectory of the spacecraft obtained using the Particle Swarm Optimization (PSO) algorithm, with each figure representing a specific phase of the mission. Figure 3 depicts the trajectory in Earth's reference frame, where the spacecraft begins at point A (departure from Earth) and transitions to point B (heliocentric transfer point), clearly showing the influence of Earth's gravity and its eventual escape into a heliocentric orbit. Figure 4 presents the trajectory in a Sun-centered inertial frame, highlighting the spacecraft's departure from Earth's orbit (Point A), its transition into the interplanetary transfer orbit initiated at Point B, and its entry into Mars's sphere of influence at Point C. The dashed green line represents the transfer trajectory, seamlessly connecting Earth's orbit with Mars's orbit, following a heliocentric conic path.

Table 4. Characterization of Relevant Points for the Refined Trajectory.

Point	Reference	Arrival Velocity (V^{arr}) [km/s]	Departure Velocity (V^{dep}) [km/s]	ΔV [km/s]
A	Earth	7.6415	11.0735	3.7860
B	Sun	32.8336	32.8342	0.0008
C	Sun	2.8726	2.6841	0.0026
D	Mars	5.2336	3.1413	2.0733

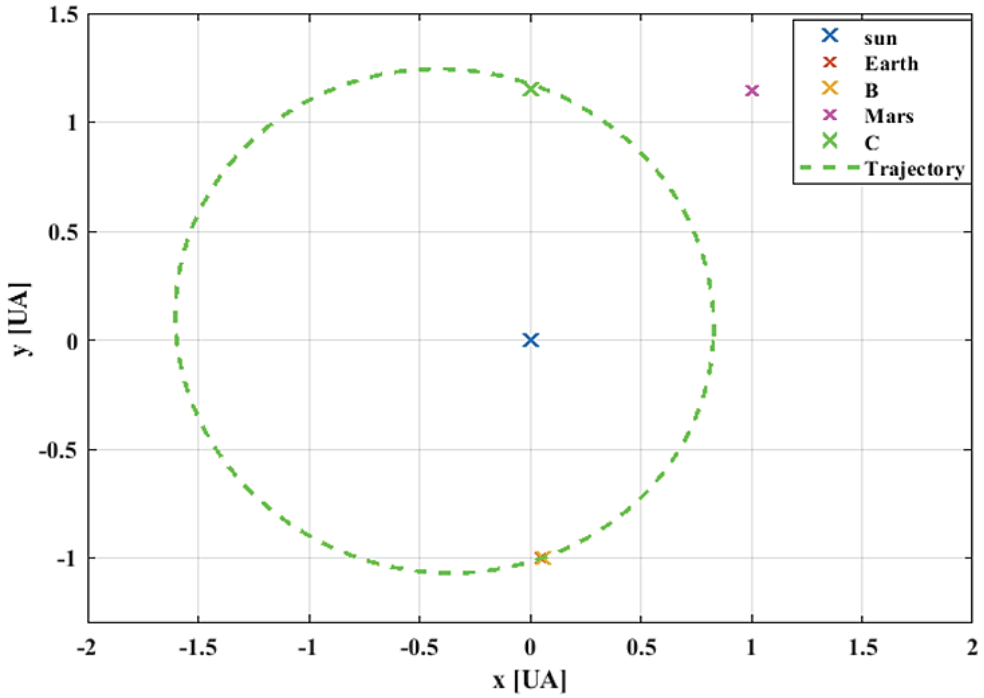

Figure 4. Trajectory in the Sun-Centered Inertial Frame

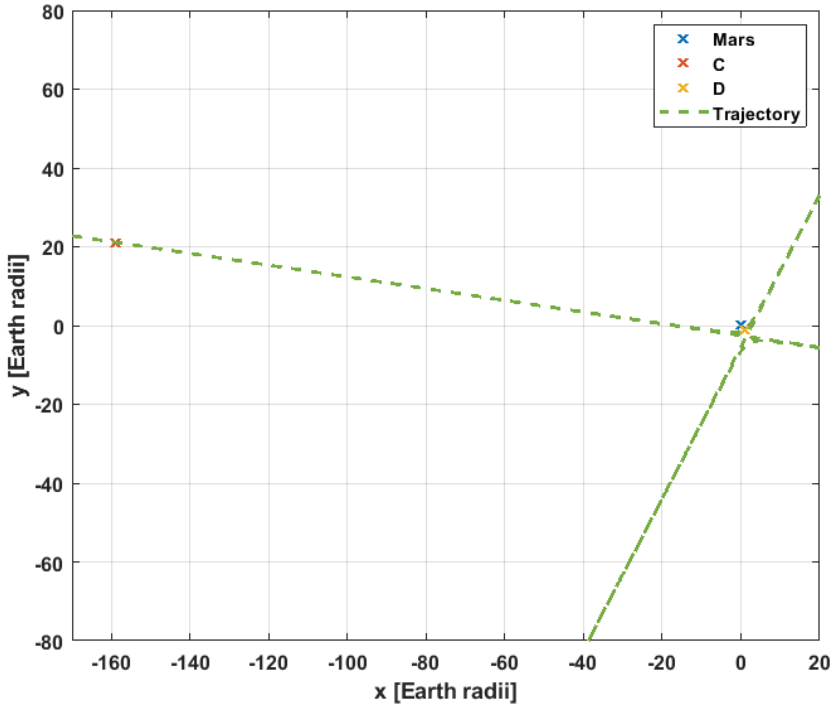

Figure 5. Mars Arrival Phase

Figure 5 provides a detailed view of the Mars arrival phase, focusing on the spacecraft's approach near Mars, where point C represents the heliocentric position before the gravity-assist maneuver, and point D indicates successful orbital insertion into Mars's sphere of influence, aligned with the arrival velocity vector Varr from Table 4. Across all figures, the trajectory confirms the consistency of the PSO-optimized solution with mission objectives, demonstrating smooth transitions between orbital phases, minimal Δv, and efficient flight times see Table 2, as well as precise alignment with the computed orbital parameters and velocity vectors from Tables 3 and 4.

Conclusion

This work underscores the significance of optimization algorithms in overcoming challenges associated with interplanetary missions and establishes a solid foundation for future research aimed at enhancing trajectory planning for multi-planetary missions. This study proposed an optimized interplanetary trajectory for a spacecraft traveling from Earth to Mars using the Particle Swarm Optimization (PSO) algorithm. The results demonstrated the PSO algorithm's effectiveness in minimizing the total Δv required for the mission while adhering to mission constraints and achieving efficient flight times. The trajectory smoothly transitions through key points—A (departure from Earth), B (heliocentric transfer initiation), C (gravity-assist near Mars), and D (Mars orbit insertion)—illustrating seamless connections between hyperbolic and elliptical orbital paths. The analysis validated the trajectory's accuracy by correlating computed values of velocity vectors, angular parameters, and conic sections (Tables 2, 3, and 4) with the visualized path in Figures 3, 4, and 5. The trajectory design successfully balances energy efficiency with flight time, highlighting the potential of PSO in solving complex space mission design problems. In future research we will focus on extending the method to multi-planet missions, integrating perturbative forces for realistic scenarios, and exploring hybrid optimization algorithms.

References

[1] Li, J., Zhao, J. and Li, F., 2018. A new method of patched-conic for interplanetary orbit. *Optik*, *156*, pp.121-127. https://doi.org/10.1016/j.ijleo.2017.10.153
[2] Miele, A., Ciarcià, M. and Mathwig, J., 2004. Reflections on the Hohmann transfer. *Journal of Optimization Theory and Applications*, *123*, pp.233-253. https://doi.org/10.1007/s10957-004-5147-z
[3] Prado, A.F.B.A., 2003. The elliptic-bi-parabolic planar transfer for artificial satellites. *Journal of the Brazilian Society of Mechanical Sciences and Engineering*, *25*(2), pp.122-128. https://doi.org/10.1590/s1678-58782003000200003.
[4] Kamel, O.M., 2009. Optimization of Bi-Elliptic transfer with plane change—Part I. *Acta Astronautica*, *64*(5-6), pp.514-517. https://doi.org/10.1016/j.actaastro.2008.10.002.
[5] Peng, L., Liang, Y. and He, X., 2025. Transfers to Earth-Moon triangular libration points by Sun-perturbed dynamics. *Advances in Space Research*, *75*(3), pp.2837-2855. https://doi.org/10.1016/j.asr.2024.10.055.
[6] Parvathi, S.P. and Ramanan, R.V., 2017. Direct transfer trajectory design options for interplanetary orbiter missions using an iterative patched conic method. *Advances in Space Research*, *59*(7), pp.1763-1774. https://doi.org/10.1016/j.asr.2017.01.023.
[7] Iwabuchi, M., Satoh, S. and Yamada, K., 2021. Smooth and continuous interplanetary trajectory design of spacecraft using iterative patched-conic method. *Acta Astronautica*, *185*, pp.58-69. https://doi.org/10.1016/j.actaastro.2021.04.021.
[8] De La Torre, D., Flores, R. and Fantino, E., 2018. On the solution of Lambert's problem by regularization. *Acta Astronautica*, *153*, pp.26-38. https://doi.org/10.1016/j.actaastro.2018.10.010.
[9] Curtis, H.D., 2021. Orbital Mechanics for Engineering Students: Revised. https://doi.org/10.1016/c2016-0-02107-1.
[10] Russell, Ryan P. "On the Solution to Every Lambert Problem,2019," Celestial Mechanics and Dynamical Astronomy 131, no. 11. https://doi.org/10.1007/s10569-019-9927-z.
[11] Vallado, David A ,*2001, Fundamentals of astrodynamics and applications*. Vol. 12. Springer Science & Business Media.
[12] Biria, A.D., 2023. The Oblate Lambert problem: geometric formulation and solution of an unperturbed, generalized Lambert problem governed by Vinti's potential. *The Journal of the Astronautical Sciences*, *70*(5), p.38. https://doi.org/10.1007/s40295-023-00388-6.
[13] Araujo, R.A.N., Winter, O.C., Prado, A.F.B.A. and Vieira Martins, R., 2008. Sphere of influence and gravitational capture radius: a dynamical approach. *Monthly Notices of the Royal Astronomical Society*, *391*(2), pp.675-684. https://doi.org/10.1111/j.1365-2966.2008.13833.x.
[14] BATE, R., MUELLER, D. and WHITE, J., 1971. Fundamentals of astrodynamics (Book on astrodynamics covering n body equations of motion, orbital elements, differential corrections, time of flight, ballistic missiles and interplanetary transport).
[15] Pontani, M. and Conway, B.A., 2012. Particle swarm optimization applied to impulsive orbital transfers. *Acta Astronautica*, *74*, pp.141-155. https://doi.org/10.1016/j.actaastro.2011.09.007.
[16] Zotes, F.A. and Penas, M.S., 2012. Particle swarm optimisation of interplanetary trajectories from Earth to Jupiter and Saturn. *Engineering Applications of Artificial Intelligence*, *25*(1), pp.189-199. https://doi.org/10.1016/j.engappai.2011.09.005.
[17] Kennedy, J. and Eberhart, R., 1995. Particle swarm optimization in: Proceedings of ICNN'95-international conference on neural networks, 1942–1948. *IEEE, Perth, WA, Australia*. https://doi.org/10.1109/icnn.1995.488968.
[18] Erdogmus, P., 2018. Introductory chapter: swarm intelligence and particle swarm optimization. *Particle swarm optimization with applications*, *10*. https://doi.org/10.5772/intechopen.74076.